Selected papers presented at the 14th Symposium of Magnetic Measurements and Modelling SMMM'2023

Investigations of Nernst Effect in Nickel Samples

Ł. Bernacki*, R. Gozdur and E. Raj

Department of Semiconductor and Optoelectronic Devices, Lodz University of Technology, Politechniki av. 10, 93-590 Lodz, Poland

Doi: 10.12693/APhysPolA.146.15 *e-mail: lukasz.bernacki@p.lodz.pl

Presented work concerns thermally activated 2D materials inducing an electric field in the presence of a magnetic field. The thermomagnetic Nernst effect combines these quantities, and several works reveal results that could be used for validation of the experimental setup before investigations of other structures with potential thermomagnetic effects. The paper shows experimental studies on the thermomagnetic Nernst effect observed in pure nickel samples. The scope of experimental studies covers relationships of the sensitivity of the Nernst coefficient to magnetic field ranging to 1 T and temperature gradient above room temperature. The obtained results were discussed in relation to the referenced works.

topics: direct current (DC), Nernst effect, thermomagnetic effect, nickel Nernst coefficient

1. Introduction

Currently, there is a trend towards sources of green energy exploitation and better energy conversion methods [1]. The article fits into these trends because it refers to the Nernst effect as the conversion of thermal energy into useful electrical energy.

The Nernst effect (NE) is a thermomagnetic phenomenon that combines thermal and electrical quantities and establishes a physical link for utilization as a direct energy converter between these two domains [2]. Thermomagnetic effects (e.g., magnetic hysteresis loop or eddy currents) are often excluded from research interest because of their dissipative and parasitic nature [3, 4]. Thermoelectric and thermomagnetic effects play a crucial role in linking thermal and electrical generators. The most popular type of thermoelectric generator is based on the Seebeck effect, which is mainly observed in semiconductors and provides good sensitivity in systems where thermoelectric generators act as sensors. The performance of these generators is still insufficient to make a breakthrough. Recent studies show that thermoelectric generators (TEGs) have the potential for further development and improvement.

A critical review of thermoelectric effects provided a breakthrough by highlighting the giant Nernst effect observed in URu_2Si_2 samples [5]. Several papers show significant values of the Nernst coefficient and achievable voltages, providing encouraging indications of materials in which the Seebeck effect is significantly higher. In paper [6], significant evidence is given that the thermal current and the electron current are compatible. Thus, in the Nernst effect, there can be a self-replication of the lift current due to the compatibility of the thermal and electron currents. In thermoelectric materials, the opposite phenomenon occurs, where the thermal current counteracts the electron current, and thus thermoelectric effects have a self-damping mechanism [7]. An interesting solution has also been presented in works [8, 9], where the authors show the combination of both thermoelectric and thermomagnetic generators [10]. The same situation occurs when observing the spin Seebeck effect (SSE), where the voltage due to SSE and the Nernst effect appear simultaneously. Very often the presented results on SSE are strongly distorted by the parasitic (NE) [3, 4]. Several papers show that NE can be used in direct energy conversion systems [11], but they do not represent a breakthrough.

There are several works showing that research is being carried out in the area of thermogenerators using the Nernst effect [3, 5]. The scientific papers do not confirm each other to determine the most promising direction for this technology. With this in mind, the authors of this paper wish to provide an overview of NE in the most commonly used nickel samples and will present a comparative analysis. The lack of convergence in the presented data leads us to attempt to revise the experimental results with our own experiment.

2. Overview of the Nernst effects

Three Nernst effects are distinguished in the scientific literature [12]. The first of these is the Nernst effect (NE). The NE is a thermomagnetic effect in which a temperature gradient in the presence of a magnetic field results in an electric field due to the deflection of diffusing electrons by the Lorentz force.

In metals, NE is the generation of a transverse electric field $\boldsymbol{E}_{\mathrm{NE}}$ when a perpendicular external magnetic field $\boldsymbol{B}_{ex}$ is applied to the sample and a temperature gradient ∇T is present in the plane of the sample (Fig. 1) [8, 9]. This means that the electric potential is attainable if the product of the field strength and the temperature gradient is non-zero and the field strength increases. The resulting electric field is expressed as the product of the magnetic field, the temperature gradient, and the Nernst coefficient Q_0 and is given by

$$\boldsymbol{E}_{\mathrm{NE}} = Q_0 \left(\boldsymbol{B}_{ex} \times \nabla T\right). \tag{1}$$

In ferromagnets, the observed electric field can contain two components that depend on the source of the magnetic field. The electric field is proportional to the external magnetic field whose origin is outside the sample. The second component is due to the intrinsic magnetization $\boldsymbol{M}$ of the residual field and is known as the anomalous Nernst effect (ANE) [13]. The resulting electric field can be expressed as

$$\boldsymbol{E} = \boldsymbol{E}_{\mathrm{NE}} + \boldsymbol{E}_{\mathrm{ANE}} = Q_0 \left(\boldsymbol{B}_{ex} \times \nabla T\right) + Q_S \left(\mu_0 \boldsymbol{M} \times \nabla T\right). \tag{2}$$

Another simplified approach is presented in paper [14], where the electric potential $\boldsymbol{E}$ is described as

$$\boldsymbol{E} = Q\, \boldsymbol{H}\, B\, \frac{\mathrm{d}t}{\mathrm{d}x}. \tag{3}$$

In this case, the dependence of the electric potential $\boldsymbol{E}$ is the result of the interactions between Nernst coefficient Q, the intensity of the magnetic field $\boldsymbol{H}$, the breadth of the specimen B, and the primary temperature gradient $\mathrm{d}t/\mathrm{d}x$. ANE is associated with high remanence materials. The obtained electric field values are usually very small, but they can be measured.

There is also the planar Nernst effect (PNE) [15], but it is not considered in this work.

Despite some significant work and the discovery of the giant Nernst effect, there has been no progress in the development of NE and related effects. On the other hand, there is no conclusive evidence that these effects are useless. TMEs are not popular because they do not represent a potential for large-scale energy conversion systems, but the continuing development of technology allows the use of micro-generation sources in ultra-low power devices where, in our opinion, these effects could find application as generation effects in energy converters.

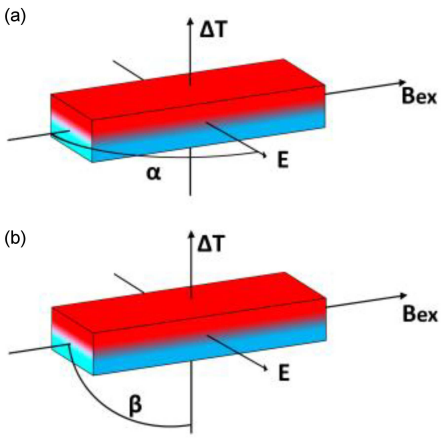

Fig. 1. The diagram of the electric potential $\boldsymbol{E}$, the intensity of the magnetic field $\boldsymbol{B}_{ex}$, and the temperature difference representing (a) the classical and anomalous Nernst effect and (b) the planar Nernst effect.

This study conducted experimental measurements of the Nernst effect (NE) in nickel and compared the results with those presented in existing publications. The current investigation extends the temperature range and enhances measurement accuracy, providing new insights into NE in nickel. While previous analyses focused on NE in pure elements, this study offers a more comprehensive understanding of the phenomenon. Papers [14, 16] provide selected measurement data and adjust a predictive curve for NE in nickel. This study aims to fill the data gap left by previous studies, which were extensive but lacked completeness and had a limited number of measurement points. Our research was carried out within the temperature range typical of human environments, and the results were compared with existing scientific data.

3. Preparation and measurements

The thermomagnetic Nernst effect was investigated in nickel samples under magnetic field excitation of 1 T in the temperature range of 263–232 K. Samples with overall dimensions $20 \times 4 \times 0.2$ mm^3 were tested in a transverse arrangement, i.e., in one in which the applied magnetic field vector was applied transversely to the temperature difference along the sample length, as shown in Fig. 1a [12]. Prior to comparative analysis, all necessary results and relevant coefficients had been normalized. Units of physical quantities were converted to be in agreement with the SI unit system.

The nanovoltmeter Agilent 34420A was used to measure the Nernst voltage. High accuracy and resolution are required as typical Nernst voltage values are in the order of a few μV [7]. The source of the

Summary of instrumentation accuracy. TABLE I

Device	Accuracy	Abs error
Lake Shore 475 DSP gaussmeter	0.05% RDG	0.3 mT
Agilent 34420A nanovoltmeter	50 ppm RDG + 20 ppm FSR	0.1 μV
Keithley DAQ6510 4-wire thermometer	0.06°C RDG	0.26°C
Omega PT100 sensor	0.2°C RDG	

constant and homogeneous external $\boldsymbol{B}_{ex}$ magnetic field is an electromagnet from Dexing Magnet, with field strengths ranging from a few mT to 2 T in the air. Lake Shore 475 DSP gaussmeter with HMMT-6J04-Vf test probe was used to measure the magnetic field applied under tests. The test bench holder consists of three pairs of voltage probes, allowing for the simultaneous measurement of up to three samples (e.g., reference samples and a tested sample). Samples under test were placed in a thermostatic chamber to ensure constant ambient temperature and the applied ΔT between two sides of the tested samples (Fig. 1). The temperature inside the chamber and ΔT were controlled using a high-performance, low-noise LTC1923 Analog Devices thermoelectric temperature controller. Temperatures were measured by means of Keithley DAQ6510 multimeter and Omega PT-100 sensors (accuracy class 1/3B). Instruments were autocalibrated, zero reference level was adjusted, and NPLC averaging was enabled. Instruments' accuracies were collected in Table I.

The process of measurement involves taking simultaneous readings from probes measuring Nernst voltages and the value of applied magnetic field strength on the surface of the test samples. At each measuring point, more than 100 measurements are taken, and the final result is the average of these measurements. The system repeatedly exposes the samples to an external magnetic field of up to 0.6 T with a fixed step throughout the cycle (Fig. 2).

4. Results and discussion

The relationships between the potential V_{NE} and biasing magnetic field $\boldsymbol{B}_{ex}$ are depicted in Fig. 3. Measurements were carried out in the steady state. The measurements were repeated a given number of times for each setup of magnetic field and temperature difference. The paper presents averaged results that demonstrate the comparable magnetization characteristics of nickel. Saturation occurs at around 50 mT, representing the maximum value achieved by the potential V_{NE}. The voltage peaks are observed at $\Delta T = 60$°C. Our findings are consistent with results published in other papers [14, 16].

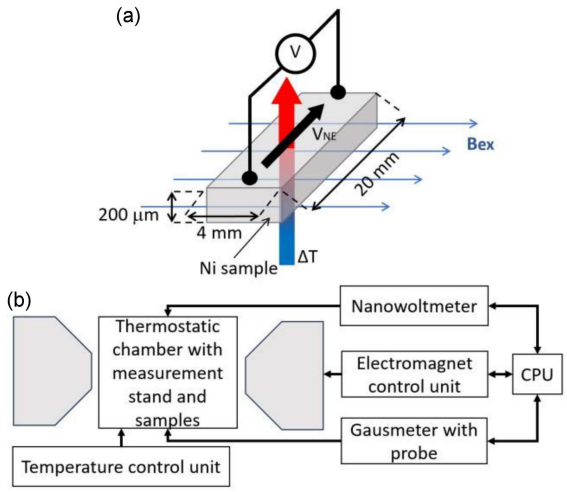

Fig. 2. The schematic diagram of (a) tested Ni sample and (b) thermostatic chamber with measurement setup.

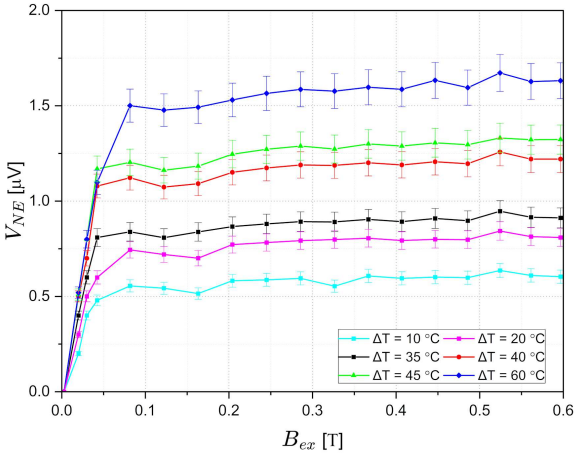

Fig. 3. The Nernst voltage as a function of the magnetic field at selected temperatures.

Figure 4a and 4b compares the obtained measurements with previously published findings [14, 16]. A.W. Smith examined two samples of pure nickel (black dashed line and blue dotted line) [16]. The red and the purple straight lines represent data obtained by the authors of the present study. The relationship between the resulting voltage V_{NE}, temperature differences ΔT, and external magnetic field strength $\boldsymbol{B}_{ex}$ are consistent with the predictions of the theory of the thermomagnetic Nernst effect in ferromagnetic materials [4]. These exhibit similar magnetization characteristics to that of nickel. Saturation transpires approximately at 40 mT, which marks the highest value attained by the voltage V_{NE}. The voltage reaches its peak at $\Delta T = 60$°C in this study, whereas A.W. Smith's research indicates that the maximum value occurs between 300–340°C, followed by a decline, which is normal and attributed to the Curie temperature. For nickel,

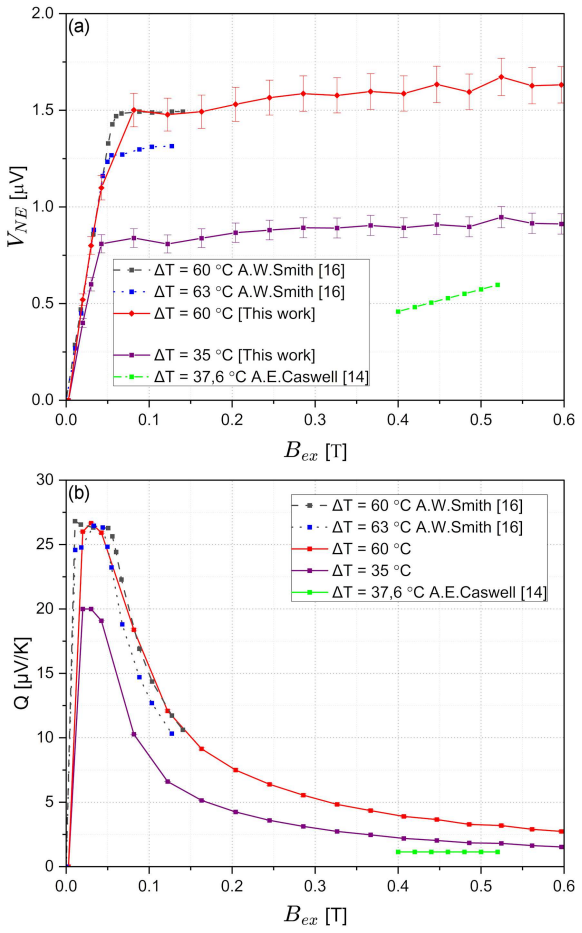

Fig. 4. The Nernst voltage as a function of the magnetic field at selected temperatures. (a) A comparison of data obtained in this work (red straight line) and data obtained by A.W. Smith [16] (black dashed and blue dotted line) and by A.E. Caswell [14] (dash-dotted green line). (b) The Nernst coefficient Q as a function of the magnetic field at temperature difference $\Delta T \sim 60$°C and $\Delta T \sim 35$°C.

the Curie temperature is about 350°C. A.E. Caswell presented data for a pure nickel sample, depicted as a green, dash-dotted line (Fig. 5).

The selected field-dependent Nernst coefficient Q for a $\Delta T \sim 60$°C is shown in Fig. 4b. The relationship in the steady state is comparable to those presented in work [16] for two different materials. An increase in temperature leads to a rise in the number of unpaired electrons, which in turn results in an increase in the material's magnetic moment. According to the Curie–Weiss law, magnetic susceptibility is proportional to the magnetic moment, and therefore, a temperature increase also causes an increase in magnetic susceptibility. At low magnetic fields, the atomic moments of Ni are chaotically oriented, leading to a linear increase in magnetic susceptibility. As the magnetic field rises, the atomic moments begin to align, resulting in a

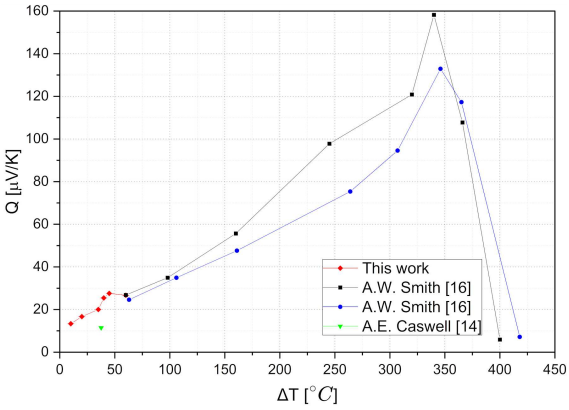

Fig. 5. A comparison of the Nernst coefficient Q as a function of temperature T obtained in this work (red rhombus) and data obtained by A.W. Smith [16] (blue circled and black squared line) and A.E. Caswell [14] (green triangulated line).

decrease in magnetic susceptibility. At sufficiently high fields, all atomic moments align, and the magnetic susceptibility reaches a saturation point [16]. The highest recorded value of Q was 26.6 μV/K at approximately 40 mT. This result was confirmed by Smith, who obtained a similar value of 26.8 μV/K under the same conditions. The difference between the two measurements was only 0.75%, which is within the permissible error of the applied nanovoltmeter.

The authors of previous studies [14, 16] have conducted measurements and fitted a curve to characterize the Nernst effect in this material. However, these investigations were not exhaustive and included only a limited number of measurement points. In contrast, our current study has undertaken comprehensive measurements across a temperature spectrum typically encountered in the human environment, which holds significant potential for thermoelectric generation applications. We observed that the maximum value of the Nernst coefficient, Q, which is 158 μV/K, was achieved at a temperature of 340 K.

5. Conclusions

The study has shown that the value of the Nernst voltage in the nickel samples is in agreement with the literature data. The investigations also show a strong dependence of the Nernst voltage on the magnetic properties of the substrates. The effect observed in nickel means that this type of substrate cannot be used in thermomagnetic generators. The experimental setup for studying the Nernst effect has been thoroughly verified, and the results are in agreement with other works. Experimental data allows for a more complete understanding of the

Nernst effect and its potential applications in energy conversion technologies. Moreover, the results may indicate a new area of application of devices using the Nernst effect as sensors.

References

[1] T.-Z. Ang, M. Salem, M. Kamarol, H. Shekhar, H.A. Nazari, N. Prabaharan, *Energy Strategy Rev.* **43**, 100939 (2022).

[2] T. Chuang, P. Su, P. Wu, S. Huang, *Phys. Rev. B.* **96**, 174406 (2017).

[3] K.I. Uchida, H. Adachi, T. Kikkawa, A. Kirihara, M. Ishida, S. Yorozu, S. Maekawa, E. Saitoh, *Proc. IEEE* **104**, 1946 (2016).

[4] H. Kannan, X. Fan, H. Celik, X. Han, J.Q. Xiao, *Sci. Rep.* **7**, 6175 (2017).

[5] R. Bel, H. Jin, K. Behnia, J. Flouquet, P. Lejay, *Phys. Rev. B* **70**, 220501(R) (2004).

[6] R. Karplus, J.M. Luttinger, *Phys. Rev.* **95**, 1154 (1954).

[7] K. Behnia, H. Aubin, *Reports Prog. Phys.* **79**, 046502 (2016).

[8] Y. Sakuraba, *Scr. Mater.* **111**, 29 (2016).

[9] S.W. Angrist, *J. Heat Transf.* **85**, 41 (1963).

[10] A. Ziabari, M. Zebarjadi, D. Vashaee, A. Shakouri, *Rep. Prog. Phys.* **79**, 095901 (2016).

[11] M. Mizuguchi, S. Nakatsuji, *Sci. Technol. Adv. Mater.* **20**, 262 (2019).

[12] E.H. Sondheimer, *Proc. R. Soc. Lond. A* **193**, 484 (1948).

[13] M. Mizuguchi, S. Nakatsuji, *Sci. Technol. Adv. Mater.* **20**, 262 (2019).

[14] A.E. Caswell, *Phys. Rev.* **20**, 280 (1922).

[15] Y. Pu, E. Johnston-Halperin, D.D. Awschalom, J. Shi, *Phys. Rev. Lett.* **97**, 036601 (2006).

[16] A.W. Smith, *Phys. Rev.* **33**, 295 (1911).